Hindawi
Journal of Chemistry
Volume 2018, Article ID 3036791, 8 pages
https://doi.org/10.1155/2018/3036791

Research Article

Theoretical Study of C_2H_5 + NCO Reaction: Mechanism and Kinetics

Nan-Nan Wu,[1,2] Shun-li OuYang,[1] and Liang Li[3]

[1]*Key Laboratory of Integrated Exploitation of Bayan Obo Multi-Metal Resources, Inner Mongolia University of Science and Technology, Baotou 014010, China*
[2]*Institute of Theoretical Chemistry, State Key Laboratory of Theoretical and Computational Chemistry, Jilin University, Changchun 130023, China*
[3]*College of Physics, Jilin University, Changchun 130012, China*

Correspondence should be addressed to Shun-li OuYang; ouyangshunli@imust.cn

Received 31 October 2017; Accepted 30 January 2018; Published 14 March 2018

Academic Editor: Frederic Dumur

Theoretical investigations are performed on mechanism and kinetics of the reactions of ethyl radical C_2H_5 with NCO radical. The electronic structure information of the PES is obtained at the B3LYP/6-311++G(d,p) level of theory, and the single-point energies are refined by the CCSD(T)/6-311+G(3df,2p) level of theory. The rate constants for various product channels of the reaction in the temperature range of 200–2000 K are predicted by performing VTST and RRKM calculations. The calculated results show that both the N and O atoms of the NCO radical can attack the C atom of C_2H_5 via a barrierless addition mechanism to form two energy-rich intermediates IM1 C_2H_5NCO (89.1 kcal/mol) and IM2 C_2H_5OCN (64.7 kcal/mol) on the singlet PES. Then they both dissociate to produce bimolecular products P_1 C_2H_4 + HOCN and P_2 C_2H_4 + HNCO. At high temperatures or low pressures, the reaction channel leading to bimolecular product P_2 is dominant and the channel leading to P_1 is the secondary, while, at low temperatures and high pressures, the collisional stabilization of the intermediate plays an important role and as a result IM2 becomes the primary product. The present results will enrich our understanding of the chemistry of the NCO radical in combustion processes.

1. Introduction

Isocyanate free radical (NCO) is an important intermediate of combustion process [1]. It is an important species in NOx compound generation from two completely different combustion sources: instant generation of NOx or Fenimore mechanism [2, 3] and NOx generation from fixed fuels of nitrogen-containing compound. NCO also plays an important role in eliminating RaReNOx and NOxOUT of NOx pollutant in smoke. All of these processes depend on adding cyanic acid ($(HONC)_3$) and urea ($(NH_2)_2CO$) into exhaust gases of combustion. The generation of HNCO is the basis of following NOx elimination by NCO. Due to considerable amounts of C, N, and O in interstellar space, people believe that NCO may exist in interstellar space and plays an important role in interstellar chemistry. Through a computation study, Chen and Ho [4] reported that NCO may have important application value in synthetic chemistry. It can generate pentabasic 1,3-oxazole which is an important compound in both synthetic chemistry [5] and biochemistry [6–9] through [3 + 2] ring addition reaction with alkyne. Considering the important significance of NCO free radical in combustion, biochemistry, synthetic chemistry, and interstellar chemistry, NCO has attracted wide research attention from chemists. NCO free radical can be generated through many important chemical reactions, such as HCN + O, CN + OH, and CN + O_2. Many experimental researches reported the reaction between NCO and different elements, including Cl, NO, NO_2, C_2H_2, C_2H_4, CH_3OH, CH_3CH_2OH, $CH_{4-n}Cl_n$, CCl_2F_2, CH_3NO_2, and so on [10–18]. Besides, there are many theoretical researches on the reaction between NCO and F, ^{3}O, OH, C_2H_2, NO, NO_2, and so on [19–24].

Alkane radical is another important free radical in combustion and atmospheric and environmental chemistry. Ethyl radical (C_2H_5) is the simplest alkane radical and can reflect oxidation characteristics of many big alkane radicals,

including alkane radicals generated by olefins. As a result, the C_2H_5 + NCO reaction drew our attention.

Only Macdonald [25] has reported an experimental research on the kinetics of the C_2H_5 + NCO reaction so far. He concluded possible reaction channels:

$$C_2H_5 + NCO \longrightarrow HNCO + C_2H_4 \quad (1a)$$

$$C_2H_5 + NCO \longrightarrow HOCN + C_2H_4 \quad (1b)$$

$$C_2H_5 + NCO \longrightarrow HCN + C_2H_4O \quad (1c)$$

$$C_2H_5 + NCO \longrightarrow C_2H_5NCO/C_2H_5OCN. \quad (1d)$$

Reaction rate constants and product outputs of the C_2H_5 + NCO reaction at the temperature range 293 ± 2 K and the pressure range 2.1~2.5 Torr have been calculated in the experiment. Variation of total reaction rate constant against pressure is expressed as $k_1 = (1.25 \pm 0.16) \times 10^{-10} + (4.22 \pm 0.35) \times 10^{-10}$ P cm^{3}molecule^{-1}s^{-1}. Rate constants of other reaction channels are $k_{1a} = (1.1 \pm 0.16) \times 10^{-10}$ cm^{3}molecule^{-1}s^{-1}, $k_{1b} = (2.9 \pm 1.3) \times 10^{-11}$, $k_{1c} = (8.7 \pm 1.5) \times 10^{-13}$ cm^{3}molecule^{-1}s^{-1} and $k_{1d} = (0.09 \pm 1.3) \times 10^{-11} + (3.91 \pm 0.27) \times 10^{-10}$ P cm^{3}molecule^{-1}s^{-1}. However, this experimental research did not study rate constant and product distribution of the C_2H_5 + NCO reaction at wider temperature and pressure ranges. Mechanism of the C_2H_5 + NCO reaction, pressure and temperature dependence of its products within a wider measuring range, and product distribution still remain unknown. As far as we know, no associated theoretical researches have been reported yet. In this paper, we carried out a comprehensive theoretical study on the C_2H_5 + NCO reaction. Its potential energy surfaces were calculated through quantum chemical calculation and its kinetics were computed using the Rice-Ramsperger-Kassel-Marcus (RRKM) unimolecular reaction rate constant theory of microcanonical ensemble. Possible isomerization and dissociation channels of products were identified, thus enabling us to get comprehensive potential energy surface information. Based on quantum chemical calculation and kinetic calculation, we got reaction rate constants and branching ratios of different reaction channels at different temperatures 200~2000 K and pressures 1–7600 Torr.

2. Calculation Methods

In this work, we employed hybrid density functional B3LYP [30, 31] method in conjunction with 6-311++G(d,p) to perform the optimization calculations of all the stationary points (including reactants, products, intermediates, and transition states) involved in C_2H_5 + NCO reaction. To obtain more reliable energetic data, single-point energy calculations were performed at the CCSD(T)/6-311+G(3df,2p) level using the B3LYP/6-311++G(d,p) optimized geometries of all the species. To characterize the nature of each stationary point, harmonic vibrational frequency calculations were performed at the same level. The local minima possess all real frequencies, whereas the transition state has one and only one imaginary frequency. The reaction path was calculated by means of intrinsic reaction coordinate (IRC) [26, 32–34] to confirm that the transition states connect designated intermediates. Unless noted, the CCSD(T) energies with inclusion of B3LYP zero-point vibrational energies (ZPE) were used throughout. All the calculations were carried out via the Gaussian 03 program packages [35].

According to the variational transition state theory (VTST) and RRKM [36] theory, the kinetic calculations for this multichannel and multiwell reaction were carried out via the MultiWell 2011 [27, 37] program on the basis of the PES obtained above in order to identify the likely mechanism and the branching ratios of various product channels.

3. Results and Discussion

3.1. Potential Energy Surface and Reaction Mechanism. The optimized geometries of the reactants, products, intermediates, and transition states for C_2H_5 + NCO reaction are shown in Figure 1, respectively, along with the available experimental data from the literature. It is found that when comparison is available, the agreement between theoretical and experimental results is good, with the largest discrepancy within a factor of 1.9%. The schematic profile of the PES is depicted in Figure 2. The total energy of the reactant R[C_2H_5 + NCO] is set to be zero for reference.

3.1.1. Initialize Connection. There are two possible initialize channels of the C_2H_5 + NCO reaction (Figures 1 and 2). N and O atoms in NCO attack C atoms in C_2H_5 to form entrance intermediates IM1 C_2H_5NCO (−89.1 kcal/mol) and IM2 C_2H_5OCN (−64.7 kcal/mol) through energy barrier-free addition reaction. Such typical initialize connection of free radicals will release abundant heat, thus making IM1 and IM2 have high chemical activity. This lays foundations for the following isomerization or dissociation. IM1 and IM2 can transform mutually through a four-membered ring transition state TS5 (−6.1 kcal/mol).

3.1.2. Dissociation Channel. Two available dissociation channels were found from IM1 C_2H_5NCO. In Figure 2, IM1 produces P_2 HNCO + C_2H_4 (−72.9 kcal/mol) through 1,3-H-transfer via a four-membered ring transition state TS1 (−17.9 kcal/mol). Alternatively, IM1 produces P_1 HOCN + C_2H_4 (−47.9 kcal/mol) through 1,5-H-transfer via a six-membered ring transition state TS2 (−31.4 kcal/mol).

Figure 2 shows that there are three feasible dissociation channels from the energy-rich intermediate IM2 C_2H_5OCN: (1) 1,3-H-transfer produces P_1 through a four-membered ring transition state TS3 (−8.7 kcal/mol); (2) synergetic 1,3-H-transfer is accompanied with C-O bond breakage and produces P_3 HCN + CH_3CHO (−66.7 kcal/mol) through a six-membered ring transition state TS6 (13.4 kcal/mol); (3) 1,5-H-transfer produces P_2 through a four-membered ring transition state TS4 (−31.9 kcal/mol).

To sum up, important theoretical dissociation channels of the C_2H_5 + NCO reaction on the CCSD(T)/6-311+G(3df,2p)//B3LYP/6-311++G(d,p) level of theory are

$$R\ C_2H_5 + NCO \longrightarrow IM1\ C_2H_5NCO \longrightarrow P_1\ HOCN + C_2H_4 \quad (2)$$

$$R\ C_2H_5 + NCO \longrightarrow IM1\ C_2H_5NCO \longrightarrow P_2\ HNCO + C_2H_4 \quad (3)$$

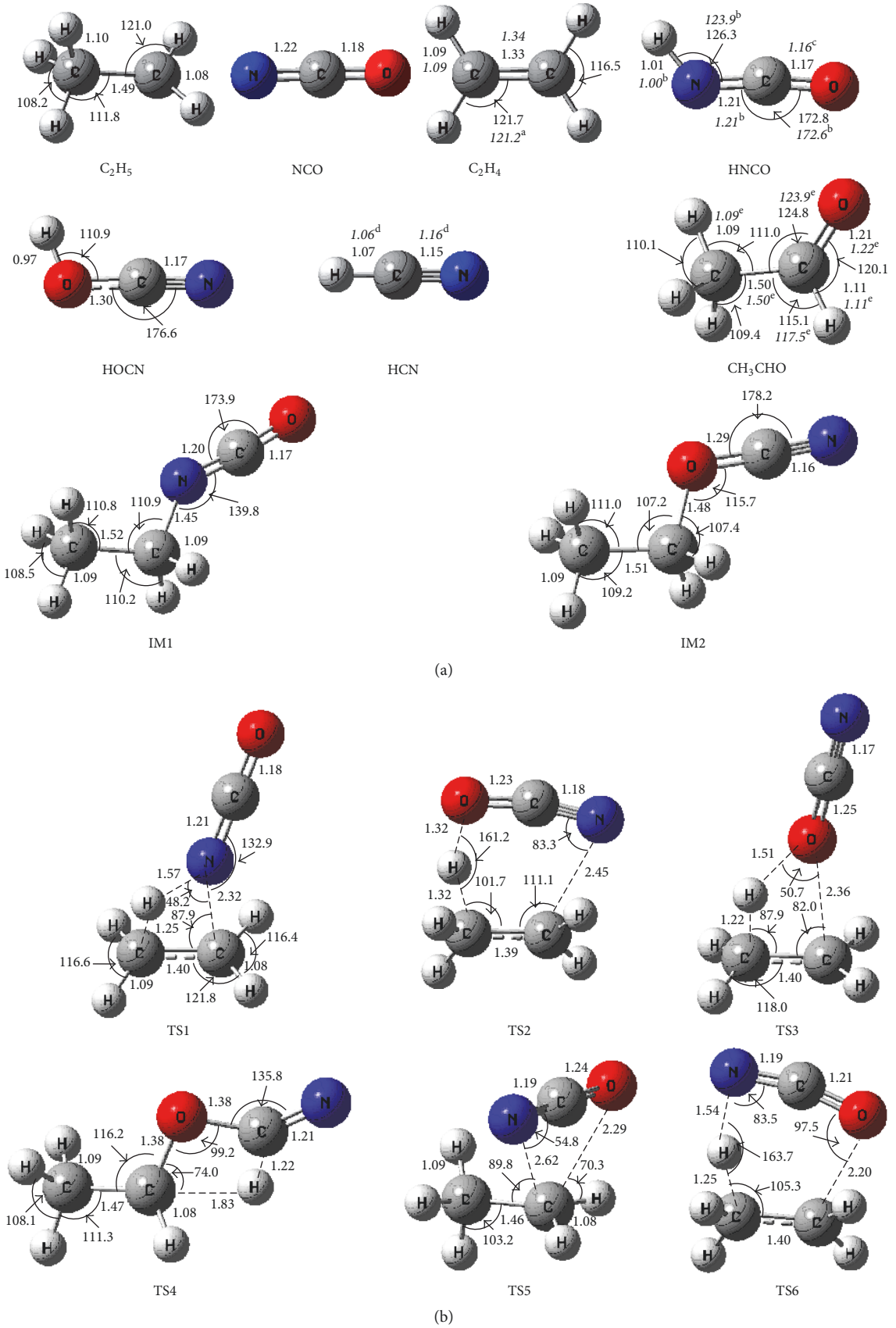

FIGURE 1: B3LYP/6-311++G(d,p) optimized geometries for the reactants, products, intermediates (IM), and the corresponding transition states (TS) of C_2H_5 + NCO reaction. The values in parentheses are the pertinent experimental data from the literature and a–e represent [26, 26–29], respectively. Bond lengths are in Å and bond angles are in degree.

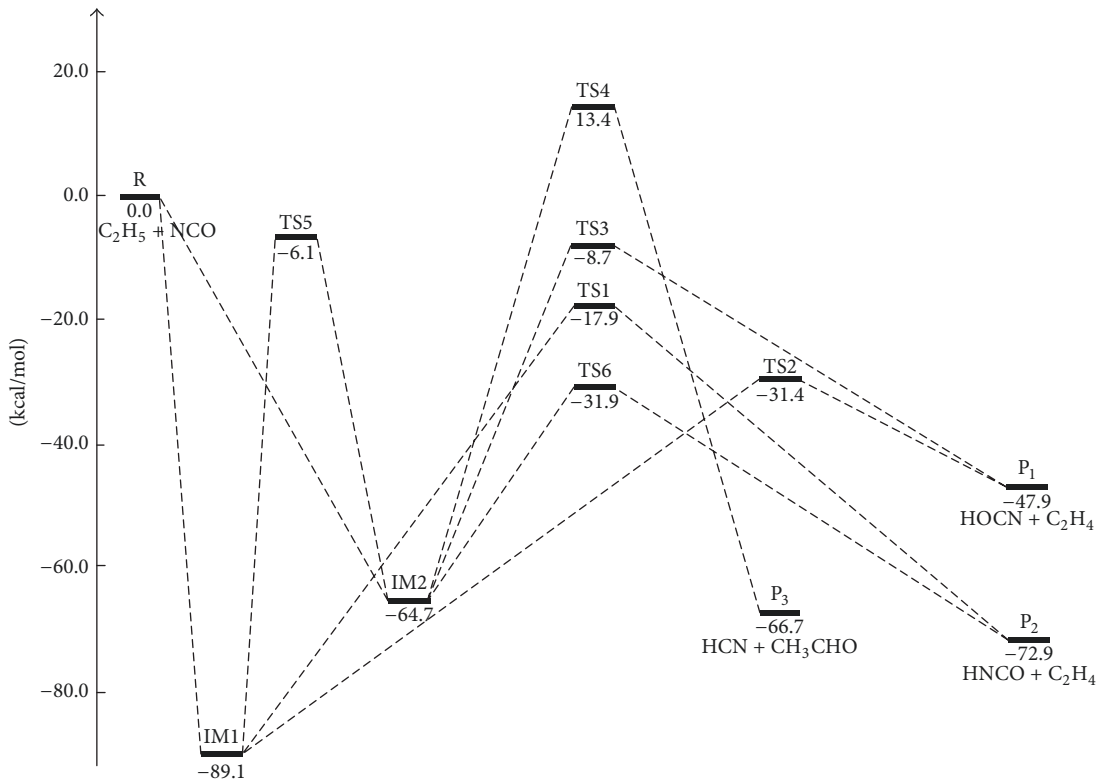

Figure 2: Schematic singlet potential energy surface of the C_2H_5 + NCO reaction at the CCSD(T)/6-311+G(3df,2p)//B3LYP/6-311++G(d,p)+ZPE level.

$$\text{R } C_2H_5 + NCO \longrightarrow \text{IM2 } C_2H_5OCN \longrightarrow P_1 \text{ } HOCN + C_2H_4 \quad (4)$$

$$\text{R } C_2H_5 + NCO \longrightarrow \text{IM2 } C_2H_5OCN \longrightarrow P_2 \text{ } HNCO + C_2H_4 \quad (5)$$

$$\text{R } C_2H_5 + NCO \longrightarrow \text{IM2 } C_2H_5OCN \longrightarrow P_3 \text{ } HCN + CH_3CHO\,. \quad (6)$$

Apparently, the rate-limiting transition state TS4 (13.4 kcal/mol) in channel (6) has far higher energy than TS2 (−31.4 kcal/mol), TS1 (−17.9 kcal/mol), TS3 (−8.7 kcal/mol), and TS6 (−31.9 kcal/mol) in previous four reaction channels. Therefore, channel (6) could not compete with the rest of the four channels and is neglected in the following kinetic calculation. Channel (5) has the lowest energy barrier (32.8 kcal/mol) and the lowest energy of P_2HNCO + C_2H_4 (−72.9 kcal/mol). It is the most feasible one in both thermodynamics and kinetics. Although channel (3) has the highest thermodynamics stability of product energy, it has to overcome a higher energy barrier (71.2 kcal/mol) than channels (2) (57.7 kcal/mol) and (4) (56.0 kcal/mol). Therefore, channel (3) could not compete with channels (2) and (4) in kinetics. Since channels (2) and (4) have the same product (P_1HOCN + C_2H_4) and similar energy barriers, they compete with each other. Moreover, intermediates IM1 and IM2 can transform mutually through high energy barriers. However, further kinetic calculation of the C_2H_5 + NCO reaction is needed to determine its product distribution and temperature and pressure dependence of its reaction rate constant at wider measuring ranges. The following text uses RRKM calculation to calculate rate constants and branching ratios of all reaction channels.

3.2. Kinetic Calculations. Based on acquired potential energy surface information of C_2H_5 + NCO reaction, rate constants of the overall reaction and multiple reaction channels as well as branching ratio of various products at the temperature range 200~2000 K and pressure range 1~7600 Torr were calculated with MultiWell 2011 program [27, 37]. Kinetic bottleneck of energy barrier-free reaction channels, for example, entrance channels of IM1 C_2H_5NCO and IM2 C_2H_5OCN with chemical activity, was identified using variational transition state theory (VTST) [38, 39]. Therefore, we carried out restricted optimization calculation by fixing length of C-N bond in IM1 C_2H_5NCO or C-O bond in IM2 C_2H_5OCN. Total single-point energy along the reaction coordinates was corrected. Energies and molecular parameters (reaction energy barrier, rotational inertia, and vibration frequency) of reactants, products, intermediates, and transition states which were calculated from ab initio were used in kinetic calculation. The total reaction rate constant (k_{tot}) is the sum of rate constants of corresponding reaction channels. At 293 K and 4 Torr, the calculated reaction rate constant of P_2HNCO + C_2H_4(k_{P2}) and reaction rate constant of P_1HOCN + C_2H_4(k_{P1}) are 2.47×10^{-10} $cm^3 molecule^{-1} s^{-1}$ and 2.50×10^{-11} $cm^3 molecule^{-1} s^{-1}$, which agrees well with Macdonald's [25] experimental results

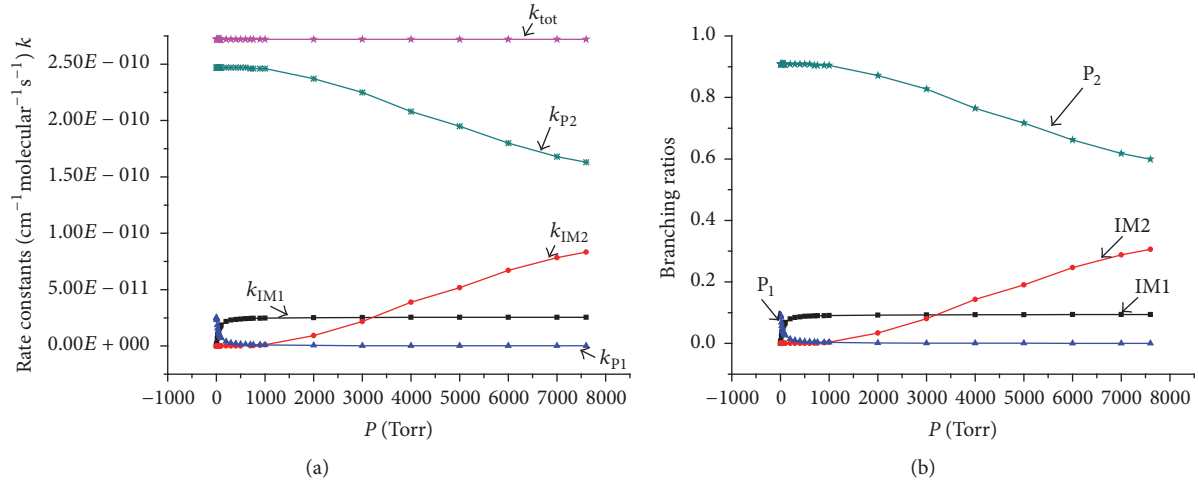

FIGURE 3: (a) Rate constants of total and various reaction channels at 293 K in a pressure range from 1 Torr to 7600 Torr. (b) Branching ratios of various reaction channels at 293 K in a pressure range from 1 Torr to 7600 Torr.

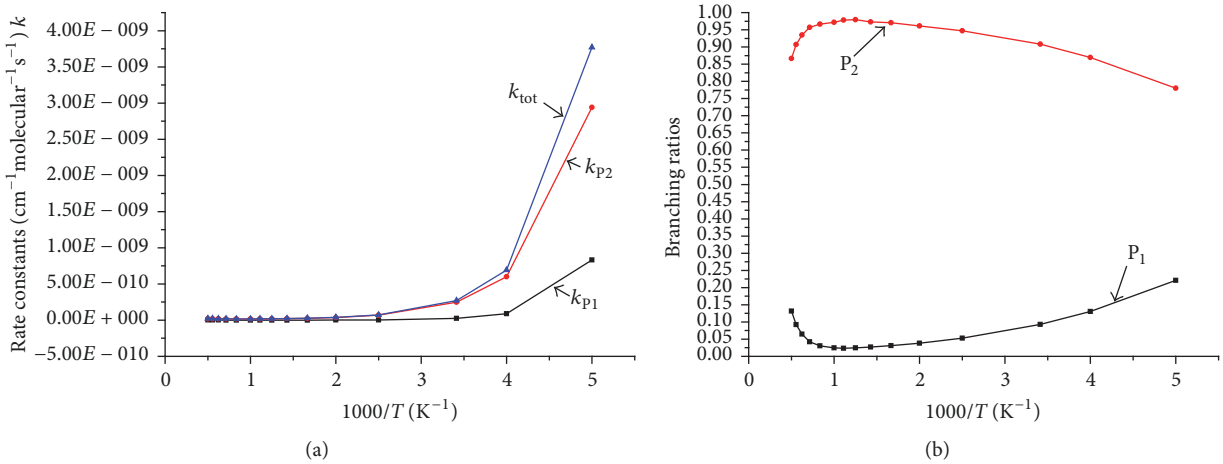

FIGURE 4: (a) Rate constants of total and various reaction channels at 1 Torr in a temperature range from 200 K to 2000 K. (b) Branching ratios of various reaction channels at 1 Torr in a temperature range from 200 K to 2000 K.

((1.1 ± 0.16) × 10^{-10} cm^{3}molecule^{-1}s^{-1} and (2.9 ± 1.3) × 10^{-11} cm^{3}molecule^{-1}s^{-1}, resp.). However, the experimental prediction of rate constant of HCN + C_2H_4O is (8.7 ± 1.5) × 10^{-13} cm^{3}molecule^{-1}s^{-1}, while the theoretical prediction is very small.

The relationship of reaction rate constants and branching ratios of reaction channels with pressure 1~7600 Torr at 293 K are shown in Figures 3(a) and 3(b). At 293 K, k_{tot} is independent of pressure. Within the whole testing pressure range, bimolecular dissociation product P_2 is the major product and k_{P2} is negatively correlated with pressure. The branching ratio of P_2 decreases from 0.91 to 0.60. When pressure < 29 Torr, P_1 becomes the secondary product and the order of rate constants of different reaction channels is $k_{P2} \gg k_{P1} > k_{IM1} > k_{IM2}$. With the increase of pressure, unimolecular product IM1 becomes the secondary product and the order of rate constants of different reaction channels is $k_{P2} \gg k_{IM1} > k_{P1} > k_{IM2}$. When pressure ≧ 3,211 Torr, IM2 becomes the secondary product and the order of rate constants of different reaction channels is $k_{P2} > k_{IM2} > k_{IM1} > k_{P1}$. When pressure < 600 Torr, IM2 decomposed into bimolecular products P_1 and P_2 completely. The output of IM2 is almost zero. As pressure increases from 1 to 600 Torr, output of IM1 increases from 0 to 0.09, while output of P_2 decreases quickly from 0.10 to 0.01. When pressure > 600 Torr, output of IM2 increases dramatically and reaches the peak 0.31 at 7600 Torr, but IM1 remains basically unchanged, close to 0.09. P_2 varies similarly to IM1 and its output remains smaller than 0.01.

The relationship of reaction rate constants and branching ratios of reaction channels with temperature 200~2000 K at 1 Torr are presented in Figures 4(a) and 4(b). When pressure = 1 Torr, impact stabilization effect of intermediates can be neglected completely. Both IM1 and IM2 transform into bimolecular product fragments P_1 and P_2 completely. k_{tot} is contributed by P_1 and P_2. In Figure 4(a), k_{tot}, k_{P1}, and k_{P2} decrease continuously before 600 K and then remain basically the same with the continuous increase of temperature. In

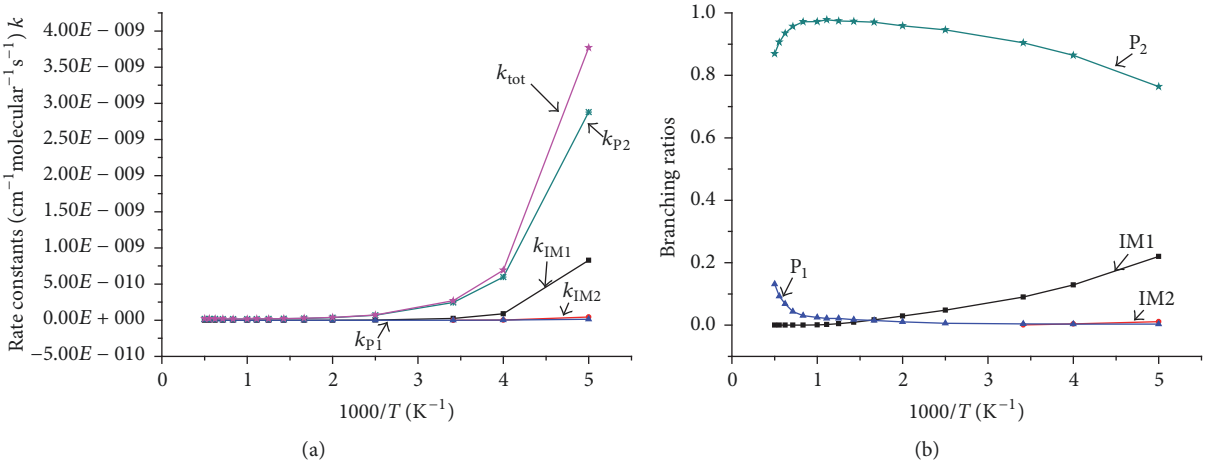

FIGURE 5: (a) Rate constants of total and various reaction channels at 760 Torr in a temperature range from 200 K to 2000 K. (b) Branching ratios of various reaction channels at 760 Torr in a temperature range from 200 K to 2000 K.

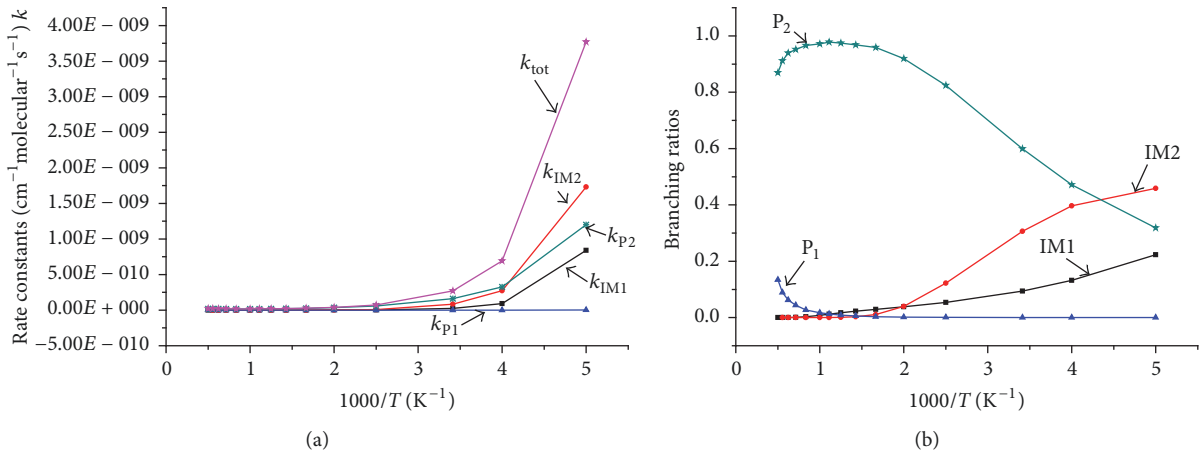

FIGURE 6: (a) Rate constants of total and various reaction channels at 7600 Torr in a temperature range from 200 K to 2000 K. (b) Branching ratios of various reaction channels at 7600 Torr in a temperature range from 200 K to 2000 K.

Figure 4(b), output of P_1 decreases from 0.22 to 0.02 as temperature increases from 200 K to 900 K, while output of P_2 increases from 0.78 to 0.98. When temperature increases from 900 K to 2000 K, output of P_1 begins to increase from 0.02 to 0.13, while output of P_2 decreases from 0.98 to 0.87.

The relationship of reaction rate constants and branching ratios of reaction channels with temperature 200~2000 K at 760 Torr are presented in Figures 5(a) and 5(b). Similarly to that in Figures 4(a) and 4(b), k_{tot}, k_{P1}, k_{P2}, k_{IM1}, and k_{IM2} all decrease continuously before 600 K and then become stable. P_2 is the main product within the studied temperature. The output of P_2 increases continuously with the temperature growth and reaches the peak 0.98 at 900 K. Later, it decreases to 0.87 at 2000 K. When temperature < 600 K, IM1 is the secondary product and its output decreases from 0.22 to 0.02 as temperature increases. The output of IM1 approaches zero as temperature increases continuously. On the contrary, output of P_1 is zero at early reaction but increases quickly since 600 K, from 0.02 at 600 K to 0.13 at 2000 K. Within this temperature range, IM2 can be neglected, because its branching ratio is smaller than 0.01.

The relationship of reaction rate constants and branching ratios of reaction channels with temperature 200~2000 K at 7600 Torr are presented in Figures 6(a) and 6(b). Combining Figures 4(a), 5(a), and 6(a), it is easy to discover that at all pressures, k_{tot}, k_{P1}, k_{P2}, k_{I1}, and k_{I2}, are inversely proportional to temperature before 600 K and become independent of temperature after 600 K. In Figure 6(b), outputs of unimolecular products IM1 and IM2 decrease with the increase of temperature, while output of bimolecular product P_1 shows the opposite. Output of P_2 increases with the increase of temperature and reaches the peak 0.98 at 900 K. When temperature < 229 K, branching ratios of different products are IM2 > P_2 > IM1 > P_1 and their branching ratios are 0.45, 0.32, 0.22, and ≈0 at 200 K. When temperature >910 K, branching ratios of different products are P_2 > P_1 > IM2 ≈ IM1, and their branching ratios are 0.87, 0.13, ≈0, and ≈0, respectively, at 2000 K.

4. Conclusions

In this paper, singlet potential energy surface of the C_2H_5 + NCO reaction is calculated on the CCSD(T)/6-311+G(3df,2p)//B3LYP/6-311++G(d,p) level of theory. Rate constants and branching ratios of its main reaction channels at 200~2000 K and 1~7600 Torr are predicted. Results demonstrate that, on singlet potential energy surface, N and O atoms in NCO can attack C atoms in C_2H_5 without energy barrier to produce energy-rich entrance intermediates IM1 C_2H_5NCO (89.1 kcal/mol) and IM2 C_2H_5OCN (64.7 kcal/mol). IM1 and IM2 can be further decomposed into $P_1C_2H_4$ + HOCN and $P_2C_2H_4$ + HNCO through H-transfer. According to the kinetic calculation, we find that, within the whole studied pressure range, k_{tot}, k_{P1}, k_{P2}, k_{I1}, and k_{I2}, all present negative temperature dependence before 600 K but then become independent from temperature. At low pressure or high temperature, impact stabilization effect of intermediates can be neglected, and bimolecular product P_2 is the major product (the maximum branching ratio is 0.98), while P_1 is the secondary product (the maximum branching ratio is 0.22). At high pressure and low temperature, stabilization effect of intermediate is important and IM2 is the major product (the maximum branching ratio is 0.45). At 293 K, k_{tot} shows no obvious pressure dependence. Within the whole testing pressure range, bimolecular product P_2 is the major product, which agrees with experimental results. Furthermore, output of P_2 is negatively correlated with pressure, decreasing from 0.91 at 1 Torr to 0.60 at 7600 Torr. These research results not only have important significance to get a deeper understanding of mechanism and kinetics of the C_2H_5 + NCO reaction but also can provide references for future associated theoretical and experimental studies.

Conflicts of Interest

The authors declare that there are no conflicts of interest.

Authors' Contributions

Nan-Nan Wu and Shun-Li OuYang designed the research, performed the experimental work, and wrote the manuscript. Shun-Li OuYang provided direction and contributed to the revisions of the manuscript. Liang Li read and approved the final manuscript.

Acknowledgments

This work was supported by the National Natural Science Foundation of China (nos. 21363013, 11364027, and 11564031), the Innovation Foundation of Inner Mongolia University of Science and Technology, China (nos. 2014QNGG09 and 2015QDLQ14), Program for Young Talents of Science and Technology in Universities of Inner Mongolia Autonomous Region, China (no. NJYT-17-B10), and the Special Foundation of Instrument Research and Development in Inner Mongolia University of Science and Technology, China (no. 2015KYYQ06).

References

[1] J. A. Miller and C. T. Bowman, "Propene oxidation at low and intermediate temperatures: a detailed chemical kinetic study," *Progress in Energy and Combustion Science*, vol. 15, p. 277, 1989.

[2] N. N. Wu, *Theoretical Investigations on the Degradation Mechanisms for Several Peroxide, Carbonaceous and Nitrogenous Radicals in the Atmosphere*, Jilin university, Changchun, China, 2011.

[3] C. P. Fenimore, "Formation of nitric oxide in premixed hydrocarbon flames," *Symposium (International) on Combustion*, vol. 13, no. 1, pp. 373–380, 1971.

[4] H.-T. Chen and J.-J. Ho, "Theoretical Study of NCO and RCCH (R = H, CH_3, F, Cl, CN) [3 + 2] Cycloaddition Reactions," *The Journal of Physical Chemistry A*, vol. 107, no. 38, pp. 7643–7649, 2003.

[5] A. Meyers, *Heterocycles in Organic Synthesis*, Wiley, New York, NY, USA, 1974.

[6] D. G. I. Kingston, M. X. Kolpak, J. W. LeFevre, and I. Borup-Grochtman, "Biosynthesis of antibiotics of the virginiamycin family. 3. Biosynthesis of virginiamycin M1," *Journal of the American Chemical Society*, vol. 105, p. 5106, 1983.

[7] A. I. Meyers and R. A. Amos, "Studies directed toward the total synthesis of streptogramin antibiotics. Enantiospecific approach to the nine-membered macrocycle of griseoviridin," *Journal of the American Chemical Society*, vol. 102, no. 2, pp. 870–872, 1980.

[8] A. I. Meyers, J. P. Lawson, and D. R. Conver, "Highly stereoselective route to (E)-allyl amines via vinyltri-n-butylphosphonium salts (Schweizer reaction)," *The Journal of Organic Chemistry*, vol. 46, no. 15, pp. 3119–3123, 1981.

[9] A. I. Meyers, J. P. Lawson, D. G. Walker, and R. J. Linderman, "Synthetic studies on the streptogramin antibiotics. Enantioselective synthesis of the oxazole dienyl amine moiety," *The Journal of Organic Chemistry*, vol. 51, no. 26, pp. 5111–5123, 1986.

[10] Y. Gao and R. G. Macdonald, "Determination of the Rate Constants for the NCO($X^2\Pi$) + Cl(^2P) and Cl(^2P) + ClNCO(X^1A') Reactions at 293 and 345 K," *The Journal of Physical Chemistry A*, vol. 109, no. 24, pp. 5388–5397, 2005.

[11] W. F. Cooper, J. Park, and J. F. Hershberger, "Product channel dynamics of the cyanato radical + nitric oxide reaction," *The Journal of Physical Chemistry C*, vol. 97, no. 13, pp. 3283–3290, 1993.

[12] D. Y. Juang, J. Lee, and N. S. Wang, "Kinetics of the reactions of NCO with NO and NO_2," *International Journal of Chemical Kinetics*, vol. 27, no. 11, pp. 1111–1120, 1995.

[13] C. Hu, Z. Zhu, L. Pei, Q. Ran, Y. Chen, and C. Chen, "Time-resolved kinetic studies on quenching of NCO ($A^2\sum^+$) by alkanes and substituted methane molecules," *The Journal of Chemical Physics*, vol. 118, no. 12, pp. 5408–5412, 2003.

[14] L. S. Pei, C. G. Hu, Y. Z. Liu, Z. Q. Zhang, Y. Chen, and C. X. Chen, "Kinetic studies on reactions of NCO($X\,^2\Pi^i$) with alcohol molecules," *Chemical Physics Letters*, vol. 381, no. 1-2, pp. 199–204, 2003.

[15] S. Wategaonkar and D. W. Setser, "The fluorine atom + isocyanic acid reaction system: a flow reactor source for isocyanate radical(~X2.PI.) and nitrogen monofluoride(X3.SIGMA.-)," *The Journal of Physical Chemistry C*, vol. 97, no. 39, pp. 10028–10034, 1993.

[16] J. Park and J. F. Hershberger, "Kinetics of NCO + hydrocarbon reactions," *Chemical Physics Letters*, vol. 218, no. 5-6, pp. 537–543, 1984.

[17] K. H. Becker, R. Kurtenbach, F. Schmidt, and P. Wiesen, "Temperature and pressure dependence of the NCO + C2H2 reaction," *Chemical Physics Letters*, vol. 235, no. 3-4, pp. 230–234, 1995.

[18] K. H. Becker, R. Kurtenbach, and P. Wiesen, "Kinetic study of the NCO + C_2H_4 reaction," *The Journal of Physical Chemistry C*, vol. 99, no. 16, pp. 5986–5991, 1995.

[19] Z.-Y. Zhou, L. Guo, and H.-W. Gao, "Theoretical studies on the mechanism and kinetics of the reaction of F atom with NCO radical," *International Journal of Chemical Kinetics*, vol. 35, no. 2, pp. 52–60, 2003.

[20] Y. Gao and R. G. Macdonald, "Determination of the rate constant for the NCO($X^2\prod$) + O(^{3}P) reaction at 292 K," *The Journal of Physical Chemistry A*, vol. 107, no. 23, pp. 4625–4635, 2003.

[21] R. Zhu and M. C. Lin, "The NCO + NO reaction revisited: Ab initio MO/VRRKM calculations for total rate constant and product branching ratios," *The Journal of Physical Chemistry A*, vol. 104, no. 46, pp. 10807–10811, 2000.

[22] Z.-G. Wei, X.-R. Huang, Y.-B. Sun, S.-W. Zhang, and C.-C. Sun, "A theoretical study on the potential energy surface of the NCO + NO 2 reaction," *Journal of Molecular Structure: THEOCHEM*, vol. 679, no. 1-2, pp. 101–106, 2004.

[23] P. Campomanes, I. Menéndez, and T. L. Sordo, "A theoretical study of the ^{2}NCO + ^{2}OH reaction," *The Journal of Physical Chemistry A*, vol. 105, no. 1, pp. 229–237, 2001.

[24] H.-T. Chen and J.-J. Ho, "Theoretical Study of Reaction Mechanisms for NCX (X = O, S) + C $_2H_2$," *The Journal of Physical Chemistry A*, vol. 107, no. 36, pp. 7004–7012, 2003.

[25] R. G. Macdonald, "Determination of the rate constant and product channels for the radical-radical reaction NCO + C_2H_5," *Physical Chemistry Chemical Physics*, vol. 9, no. 31, pp. 4301–4314, 2007.

[26] Y. Q. Tang, *Principles of Chemical Kinetics and Chemical Reactors*, Science Press, Beijing, China, 1974.

[27] J. R. Barker, T. L. Nguyen, J. F. Stanton, C. Aieta, M. Ceotto, F. Gabas et al., *MultiWell Program Suite*, University of Michigan, 2007, http://aoss.engin.umich.edu/multiwell/.

[28] S. S. Brown, H. L. Berghout, and F. F. Crim, "Raman spectroscopy of the N–C–O symmetric (ν3) and antisymmetric (ν2) stretch fundamentals in HNCO," *The Journal of Chemical Physics*, vol. 107, no. 23, pp. 9764–9771, 1997.

[29] A. L. L. East, C. S. Johnson, and W. D. Allen, "Characterization of the X 1A′ state of isocyanic acid," *The Journal of Chemical Physics*, vol. 98, no. 2, pp. 1299–1328, 1993.

[30] A. D. Becke, "Density-functional thermochemistry. III. The role of exact exchange," *The Journal of Chemical Physics*, vol. 98, no. 7, pp. 5648–5652, 1993.

[31] P. J. Stephens, F. J. Devlin, C. F. Chabalowski, and M. J. Frisch, "Ab Initio calculation of vibrational absorption and circular dichroism spectra using density functional force fields," *The Journal of Physical Chemistry C*, vol. 98, no. 45, pp. 11623–11627, 1994.

[32] Z. T. Huang, *Basic Theoretical Basis of Organic*, Chemical Industry Press, Beijing, China, 1980.

[33] JiLin University, etc. Physical Chemistry (II), Beijing: People's Education Press, 1979.

[34] D. J. Hucknall, *Chemistry of Hydrocarbon Combustion*, Springer, Dordrecht, Netherlands, 1985.

[35] M. J. Frisch, G. W. Truck, H. B. Schlegel et al., *GAUSSIAN 03*, Revision A.1, Guassian, Inc., Pittsburgh, Pa, USA, 2003.

[36] K. A. Holbrook, M. J. Pilling, and S. H. Robertson, *Unimolecular Reactions*, Wiley, Chichester, UK, 1996.

[37] J. R. Barker, "Multiple-well, multiple-path unimolecular reaction systems. I. MultiWell computer program suite," *International Journal of Chemical Kinetics*, vol. 33, no. 4, pp. 232–245, 2001.

[38] S. J. Klippenstein, "An efficient procedure for evaluating the number of available states within a variably defined reaction coordinate framework," *The Journal of Physical Chemistry C*, vol. 98, no. 44, pp. 11459–11464, 1994.

[39] S. J. Klippenstein, "A bond length reaction coordinate for unimolecular reactions. II. Microcanonical and canonical implementations with application to the dissociation of NCNO," *The Journal of Chemical Physics*, vol. 94, article 6469, 1991.